Self-diffusion of interacting micelles: FRAPP study of micelles self-diffusion

D. Chatenay, W. Urbach,[a] R. Messager, and D. Langevin
Laboratoire de Spectroscopie Hertzienne de l'ENS, associé au CNRS (U.A. 18), 24, rue Lhomond, 75231 Paris Cedex 05, France

(Received 8 July 1986; accepted 29 October 1986)

We have studied self-diffusion in DTAB micellar systems at three different salinities with fluorescence photobleaching experiments. In order to characterize interactions in these systems, we have also performed light scattering experiments. Despite of the strong variation of the interactions with salinities, almost no salinity variation in self-diffusion coefficients vs droplets volume fraction curves has been observed. A clear difference between the friction coefficients involved in self- and mutual diffusion have been evidenced.

I. INTRODUCTION

The dynamic behavior of colloidal systems has been the subject of a great number of both theoretical and experimental work these past few years. Since the works of Batchelor,[1] Ackerson,[2] and Felderhof,[3] much effort has been devoted to a better treatment of hydrodynamic interactions,[4,5] to the understanding of the behavior of concentrated systems,[5] and of the long time behavior of colloidal systems.[6,7] Classical quasielastic light scattering experiments (QELS), first performed on latex spheres or biomolecules,[9] such as protein or viruses, have been extended to various systems such as microemulsions[10] or micelles.[11,12] Those systems have been shown not only to be of valuable interest by their own but also to be interesting for comparison with theories. Indeed because the size of the suspended particles in those media (20–50 Å) is much smaller than the light wavelength (5000 Å), QELS experiments can be performed up to 50% volume fraction of particles without the commonly encountered problems of multiple scattering.[10] Furthermore, it is also relatively easy to control the interaction potentials between particles in these systems and to obtain a variety of behavior: hard sphere repulsion, shielded Coulombic repulsion, and van der Waals attraction. The major drawback of these systems is that, since they are association colloids, one has to take care of exchange times of the constituents[13] and to be aware of possible structural changes in the concentration domain under study.[11]

In contrast to the collective behavior (collective diffusion coefficient) widely studied, relatively few works have been devoted to single particle properties. Even in the simplest case of hard sphere potential, the value of the first virial coefficient of the long time self-diffusion coefficient is not definitely settled.[14] For other interaction potentials, first theoretical predictions have been done only recently.[15,16] There are few experimental results dealing with short[17] and long time self-diffusion coefficients and to our knowledge no systematic investigation of the effects of interactions on these diffusion coefficients have yet been published.

Moreover, there is still some dispute concerning the comparison of the two friction terms involved in the collective diffusion coefficient and the long time self-diffusion one.[18,19]

Thus our interest in the present paper will be mainly devoted to the measurement of long time self-diffusion coefficients in micellar solutions using fluorescence recovery after fringe pattern photobleaching (FRAPP). Light scattering experiments (both static and dynamic) are used to characterize interactions in the studied systems and their combination with self-diffusion results will allow us to discuss the problem of friction coefficients.

II. THEORETICAL BACKGROUND

A. Time and length scales in colloidal suspensions

Let us first recall briefly the time and length scales involved in Brownian motion of interacting particles. Following Pusey,[20] one may define two characteristic times. The shortest one, τ_B, is defined as the relaxation time of the Brownian particles velocity and its order of magnitude is given by[20]

$$\tau_B \sim \frac{M}{f},$$

where M is the mass of the particles and f its friction coefficient. For micellar systems, $\tau_B \sim 10^{-12}$ s. Thus all the experiments discussed below will be in the time domain $\tau \gg \tau_B$. For particles interacting via repulsive potential, a second important characteristic time can be introduced, corresponding to the renewal of the local structure induced by repulsive interactions. The range of this local ordering is roughly of the order of the interparticle separation d given by

$$d \sim 2R\Phi^{-1/3},$$

where R is the particle radius and Φ their volume fraction. For micellar systems, one has $d \sim 200$ Å. One may then define a "local structure lifetime" τ_I as the time needed for a particle to move over a distance which is roughly d. An order of magnitude for τ_I is given by

$$\tau_I \sim \frac{d^2}{6D_0},$$

where D_0 is the free particle diffusion coefficient. Typical values of τ_I are in the range of 10^{-6} s for systems considered here. Thus long time behavior must be understood as long compared to τ_I. This will be the case for self-diffusion experiments, but light scattering ones are performed in the opposite limit, i.e., for times τ such as $\tau_B \ll \tau \ll \tau_I$.

Finally let us note that the interparticle spacing defines a

[a] Also at Biophysical Lab, UER Cochin Port-Royal, 75674 Paris Cedex 14, France (ERA 593 CNRS).

 0021-9606/87/042343-09$02.10

wave vector q^* roughly given by

$$q^* \sim \frac{1}{d}.$$

In our case one has $q^* \sim 10^6\ \mathrm{cm}^{-1}$, so that all optical experiments are performed at $q \ll q^*$, i.e., well below the first peak of the structure factor. Thus all the results obtained are in the limit $q \to 0$.

B. Light scattering experiments

1. Static scattering

In the case of identical particles, the excess scattered light is proportional[21] to $P(q)\,S(q)$, where $P(q)$ is the particle form factor and $S(q)$ the time average structure factor of the solution defined by

$$S(q) = 1 + 4\pi\rho \int_0^\infty r^2 [g(r) - 1] \frac{\sin qr}{qr} dr$$

with ρ the number density of particles and g the radial distribution function. The scattering wave vector q is given by

$$q = \frac{4\pi n}{\lambda} \sin\frac{\theta}{2},$$

where n is the sample refractive index, λ the vacuum light wavelength, and θ the scattering angle.

In our case, since typical micellar radii are of order 20 Å, we have $P(q) = 1$. Having in mind the discussion above about orders of magnitude (see Sec. II A), one may set $q = 0$. Thus no anisotropy of the scattered light is observed and static experiments provide a measurement of $S(0)$, i.e., the osmotic compressibility of the system.[22] The excess scattered intensity may then be written[22]

$$I(\Phi) = GkT \left(\frac{\partial n}{\partial \Phi}\right)^2 \Phi \left(\frac{\partial \Pi}{\partial \Phi}\right)^{-1}, \tag{1}$$

where G is an instrumental constant, k the Boltzmann constant, T the absolute temperature, n the sample refractive index, Φ the volume fraction of the dispersed phase, and Π the osmotic pressure.

Low Φ variation of the scattered intensity is used to determine the micelles radii and the first virial coefficient of the osmotic pressure[22]; writing

$$\Pi = \frac{kT}{v} \Phi \left(1 + \frac{B}{2}\Phi\right), \tag{2}$$

where $v = 4\pi/3\ R^3$ is the micellar volume and B the first virial coefficient of π, one gets

$$\frac{\Phi}{I} = \frac{1}{G} \left(\frac{\partial n}{\partial \Phi}\right)^{-2} \frac{1}{v} (1 + B\Phi). \tag{3}$$

The first virial coefficient B is related to the interaction potential $V(r)$ by

$$B = \frac{1}{v} \int_0^\infty (1 - e^{-V(r)/KT}) 4\pi r^2\, dr,$$

with r center to center distance between particles.

For more concentrated solutions, one may also account for the behavior of the scattered intensity using perturbation treatment of the osmotic pressure.[23] This consists in writing the osmotic pressure as the sum of a hard sphere term Π_{HS} and a perturbation one, Π_P. The hard sphere term has the form[24]

$$\Pi_{HS} = \frac{kT}{v_{HS}} \Phi_{HS} \left[1 + \Phi_{HS} + \Phi_{HS}^2 - \Phi_{HS}^3\right] / \left[1 - \Phi_{HS}\right]^3,$$

where v_{HS} and Φ_{HS} are, respectively, the hard sphere volume and the hard sphere volume fraction. The perturbation term Π_P has the form

$$\Pi_P = \frac{kT}{v} \frac{A}{2} \Phi^2,$$

where A is related to the perturbation potential V_P (added to the hard sphere one) by[23]

$$A = \frac{4\pi}{kT} \frac{1}{v} \int_{2R_{HS}}^\infty V_P(r) r^2\, dr.$$

This treatment is valid as long as the interaction potential V_P is small, i.e., $V_P \ll kT$. Within this treatment, the first virial coefficient of the osmotic pressure becomes

$$B' = 8\left(\frac{\Phi_{HS}}{\Phi}\right) + A. \tag{4}$$

We will conclude this chapter with a few words about interaction potentials in micellar systems. Most of the trends observed in light scattering experiments on those systems are accounted for by usual theory for colloid stability[12] (DLVO theory[25]). This consists in writing the interaction potential V_P as the sum of two terms: an attractive potential V_{vdW} due to van der Waals forces and a repulsive one, V_{el}, due to shielded Coulombic repulsions. The expression of V_{vdW} for the case of two spheres of radius R is

$$V_{vdW} = -\frac{H}{12}\left[(x^2 + 2x)^{-1} + (x+1)^{-2} + 2\ln\frac{x^2 + 2x}{(x+1)^2}\right],$$

where H is the Hamaker constant and $x = (r - 2R)/R$. The electrostatic contribution can be written explicitly if the surface energy of the unit charge $e\psi_0$ is small compared to kT (here ψ_0 is the surface potential). In such a case, one has two limiting expressions for the case of two spheres:

$$KR \ll 1, \quad V_{el}(x) = \frac{q^2 e^2}{2\epsilon R(1 + KR)^2} \frac{e^{-2KRx}}{1 + x},$$

$$KR \gg 1, \quad V_{el}(x) = \frac{\epsilon R \psi_0^2}{2} \ln\left[1 + e^{-2KRx}\right],$$

where ϵ is the dielectric constant of the medium surrounding the micelles qe their electric charge and K the Debye–Hückel reciprocal length defined by

$$K = 8\pi c_s e^2 z^2 / \epsilon kT$$

with c_S concentration of ionic species in solution (ions/cm^3) and z the valence of these species.

2. Dynamic light scattering

These experiments provide a measurement of the modulus of the normalized scattered electrical field corrrelation function $|g^1(q,\tau)|$ given by[20]

$$|g^1(q,\tau)| = \frac{F(q,\tau)}{S(q)}, \tag{5}$$

where $F(q,\tau)$ is the full dynamic structure factor. In the case of N identical spherical particles[20] (whose size is small compared to the light wavelength):

$$F(q,\tau)=\frac{1}{N}\sum_{j=1}^{N}\sum_{k=1}^{N}\langle e^{i\mathbf{q}\cdot[\mathbf{r}_j(t)-\mathbf{r}_k(t+\tau)]}\rangle \tag{6}$$

and

$$F(q,0)=S(q).$$

Here $\mathbf{r}_j(t)$ is the position of the center of particle j at time t and the angular brackets indicate an ensemble average.

Depending upon the time and length scales probed by an experiment $|g^1(q,\tau)|$ may take several limiting expressions and lead to the measurements of various diffusion coefficients. We shall briefly review these different situations.

Let us start with the experiments performed at $q \ll q^*$. In that case, one may obtain a small time expansion for $|g^1(q,\tau)|^2$:

$$\ln|g^1(q,\tau)| \sim 1 - D_c q^2 \tau, \quad \tau_B \ll \tau \ll \tau_I,$$

where D_c is an effective diffusion coefficient given by[2]

$$D_c(q)=D_0\frac{H(q)}{S(q)}.$$

In this expression, D_0 is the free particle diffusion coefficient and $H(q)$ represents the contribution of hydrodynamic interactions. Since in our case we have shown that $q \sim 0$, we obtain[22]

$$D_c(\Phi)=\frac{V}{f_c(\Phi)}\frac{\partial \Pi}{\partial \Phi}, \tag{7}$$

where f_c is the friction coefficient which takes into account hydrodynamic interactions. At longer times (i.e., $\tau \gg \tau_I$), memory effects have to be taken into account[6] and the behavior of $|g^1(q,\tau)|$ is more complicated.[6,7]

We will now discuss the case $q \gg q^*$. Though, as stated above (see Sec. II A), this domain is not accessible by optical experiments in the case of micellar systems, this will provide an homogeneous introduction of self-diffusion coefficients; furthermore, this q domain could be easily explored by neutron spin echo experiments. In this domain all cross terms ($i \neq j$) vanish in Eq. (6) and $S(q) = 1$; thus, expression (5) for $|g^1(q,\tau)|$ reduces to[8]

$$|g^1(q,\tau)| = \langle e^{i\mathbf{q}\cdot[\mathbf{r}_i(t)-\mathbf{r}_i(t+\tau)]}\rangle.$$

This domain probes single particle properties. Once more the existence of two time regimes leads to different behavior of $|g^1(q,\tau)|$ depending upon the comparison between τ and τ_I. One is thus led to introduce two self-diffusion coefficients[8]: a short time one for $\tau \ll \tau_I$ and a long time D_S for $\tau \gg \tau_I$. Once more memory effects have to be taken into account to calculate this long time self-diffusion coefficient. Usually D_S is expressed[19] under the following form:

$$D_S(\Phi)=\frac{kT}{f_s(\Phi)}, \tag{8}$$

where f_S is a friction coefficient.

Let us now focus on D_S and D_c variations with concentration. In the limit of zero volume fraction, one has

$$\lim_{\Phi\to 0} D_c(\Phi)=\lim_{\Phi\to 0} D_S(\Phi)=D_0=\frac{kT}{6\pi\eta R_H}, \tag{9}$$

where η is the solvent viscosity and R_H the hydrodynamic radius of the particles. For low Φ, one may write

$$D_c = D_0[1+\alpha_c\Phi], \tag{10}$$

$$D_s = D_0[1+\alpha_s\Phi], \tag{11}$$

where α_c and α_S are the first virial coefficients and contain contributions of both direct and hydrodynamic interactions. In the case of D_c, this is obvious; indeed from Eqs. (2) and (7),

$$\alpha_c = B - \alpha_c' \tag{12}$$

with α_c' the first virial coefficient of f_c. Various treatments have been proposed in order to calculate α_c'. The more complete were those of Felderhof[3] and Batchelor[1] who obtained $\alpha_c' \simeq 6.5$ for the case of hard spheres in the low density limit assuming two body hydrodynamic interactions. These authors also gave the analytical formula allowing calculation of α_c' for any type of interaction potentials (see Ref. 10 for application to microemulsions and Ref. 12 for application to micelles). In the case of short ranged potential, α_c is related to the coefficient A obtained from the perturbation treatment described in Sec. II B 1[10]:

$$\alpha_c \sim 1{,}5 + \frac{A}{2}. \tag{13}$$

For more concentrated systems, there recently has been some attempts[26–29] taking into account four-body hydrodynamic interactions, some of them leading to somewhat different value of α_c for hard spheres.[26]

In the case of the long time self-diffusion, the discussion above about the various forms of $|g^1(q,\tau)|$, depending upon time and length scales, allows us to expect no strong dependance of D_S upon direct interaction. Indeed we have seen that in the q range where D_S can be measured, the normalization factor $S^{-1}(q)$ in expression (5) of g^1 disappears being equal to 1. In the case of hard spheres, significatively distinct values of α_S have been calculated (see Refs. 14 and 15 for a review of these values). The problem still seems open. Nevertheless, the authors of Ref. 15 have calculated α_S for attractive and repulsive potentials within the low density and two-body hydrodynamic approximations. They obtain $\alpha_S = -2$ for hard spheres and give graphs allowing the determination of α_S for other types of interactions.

III. EXPERIMENTAL RESULTS

A. Micellar systems

The surfactant we used for this study is dodecyltrimethylammonium bromide (DTAB) from Aldrich. It was twice recrystallized from ethylacetate prior to use. Molecular weight (M) and partial specific volume[30] ($\bar{v}$) are, respectively,

$$M = 308.35 \text{ g},$$

$$\bar{v} = 295.5 \text{ ml/M}.$$

Solutions were prepared in water at three distinct KBr con-

centrations: 0.5–0.1–0.01 M. All the experiments were performed at 25 °C ($\pm$ 0.1 °C).

The micellar volume fraction is then

$$\Phi = 10^{-3}(c - c^*) \times \bar{v},$$

where c is the surfactant concentration (M/ℓ) and c^* the critical micellar concentration (i.e., the concentration above which surfactant aggregation takes place). For surfactants of the DTAB type (i.e., with a 12 carbon atom chain), typical micelle lifetimes are in the range (10^{-1},10 s) depending upon surfactant and salt concentrations.[31]

B. Light scattering experiments

1. Static light scattering

All the experiments were performed at scattering angle $\theta = 90°$. Carbon tetrachloride (CCl_4) was used as a standard for calibration. For each salinity, the critical micellar concentration was obtained from these static light scattering experiments.[32] We obtained $c^* \simeq 1{,}6.10^{-3}$ M/ℓ for both 0.5 M and 0.1 M KBr solutions, and $c^* \simeq 17.10^{-3}$ M/ℓ for the 0.01 M KBr one.

For each salinity, the micellar radius R, or equivalently the aggregation number a related to R by

$$\frac{4\Pi}{3} R^3 = a \frac{\bar{v}}{N}$$

with N the Avogadro number, is determined from the plot of Φ/I vs Φ and extrapolation at $\Phi = 0$ according to Eq (3). This plot also gives the first virial coefficient of the osmotic pressure B. The way in which the perturbative treatment discussed in Sec. II B 1. is used, is described in Ref. 23.

The experimental results of scattered intensity measurements are given in Fig. 1. In this figure, the measured intensities are normalized such that $\Phi/I = 1$ for $\Phi = 0$. For 0.5 M and 0.1 M KBr, the continuous lines are obtained from the perturbation treatment described in Sec. II B 1. The agreement with experimental data is obviously excellent. The various quantities obtained from the treatment of static light scattering data are given in Table I. We may briefly sum up the obtained results:

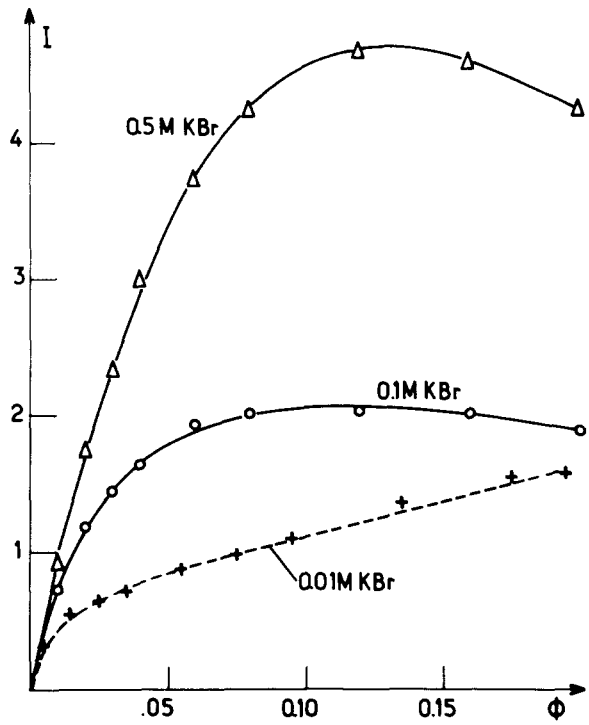

FIG. 1. Static light scattering data: scattered intensity I vs volume fraction Φ at the three studied KBr concentrations. Data are normalized so that (Φ/I) $\rightarrow$ 1 for $\Phi \rightarrow 0$. Δ:0.5 M KBr; O: 0.1 M KBr; + : 0.01 M KBr. Continous lines for 0.5 and 0.1 M KBr are the best fits obtained from perturbation treatment. Broken line for 0.01 M KBr is a guide for the eye.

(1) Increase of the aggregation number with salt concentration.

(2) Interactions between micelles are repulsive and the strength of these interactions increases as salt concentration decreases.

(3) The solutions at 0.5 M KBr behave exactly as hard spheres.

TABLE I. Parameters for the DTAB systems investigated in this work for the three distinct KBr concentrations. κ^{-1} is the Debye–Hückel length; a the aggregation number; B the first virial coefficient of osmotic pressure; and R is the mass radius. A is the coefficient related to the osmotic perturbation term; R_{HS} is the hard sphere radius; and B' is the first virial coefficient obtained using perturbation treatment. D_c^0 is the cooperative diffusion coefficient value for $\Phi = 0$, and R_H^c is the corresponding hydrodynamic radius. α^c is the first virial coefficient of D_c. D_S^0 is self-diffusion coefficient at $\Phi = 0$, R_H^S the corresponding hydrodynamic radius, and α_S the first virial coefficient of D^S.

		STATIC LIGHT SCATTERING						DYNAMIC MEASUREMENTS					
		LOW Φ BEHAVIOR			PERTURBATION TREATMENT			Q.E.L.S.			F.R.A.F.P. P.		
[K Br] (Mol/l)	K^{-1} (Å)	a	R (Å)	B	A	R_{HS} (Å)	B'	$10^7 \times D_c^0$ ($cm^2\ s^{-1}$)	R_H^c (Å)	α_c	$10^7 \times D_S^0$ ($cm^2.s^{-1}$)	R_H^S (Å)	α_S
0.01	30	43±4	17±.5	119	-	-	-				10.3±.2	23.6±.4	-5.2±.3
0.1	10	72±7	20.3±1	36	24.4	21.1	33.4	10.7±.5	22.8±1	10±1	10.4±.2	23.4±.4	-3.6±.3
0.5	4	76±7	20.7±1	8	0	20.7	8	10.7±.5	22.8±1	0±.5	10.4±.2	23.4±.4	-3.6±.3

The perturbative treatment is no longer valid in the case of 0.01 M KBr because repulsive interactions are too strong. The corresponding line in Fig. 1 is only a guide for the eye.

2. Dynamic light scattering

Dynamic light scattering experiments were performed at three scattering angles ($\theta = 90°$, 45°, 30°) in order to check the q^{-2} dependence of the initial decay time of the scattered electrical field correlation function. We have used a laboratory built autocorrelator. The autocorrelation function is measured in 105 points grouped in four zones with different sampling times. This allows us the precise determination of both the short time and asymptotic behavior ($\tau \to \infty$) of the autocorrelation function in the same run. Cumulant methods[33] were used to analyze the short time behavior. Typical decay times are in the range of the microsecond.[34] In view of the micellar lifetimes given above, micelles may be considered as permanent spheres for these experiments.

In Fig. 2, we have plotted the measured values of D_c vs Φ for the three studied KBr concentrations. The infinite dilution values of D_c (D_c^0), hydrodynamic radii (R_H^c), and first virial coefficients of D_c (α_c) are given in Table I for 0.5 M and 0.1 M KBr only; in the case of 0.01 KBr, because of the steep increase of D_c vs Φ, the determination of these values would have been much too imprecise.

For each salinity, the polydispersity index deduced from cumulant method stays low ($\sim 5\%$) in the whole studied concentration range. This confirms previous results[38,41] which have shown that the width of the size distribution curve is fairly small; from the data of Ref. 41, one may estimate that the relative dispersion of micelles radii is about 4% (this is quite comparable to the size dispersion of latex particles[46]).

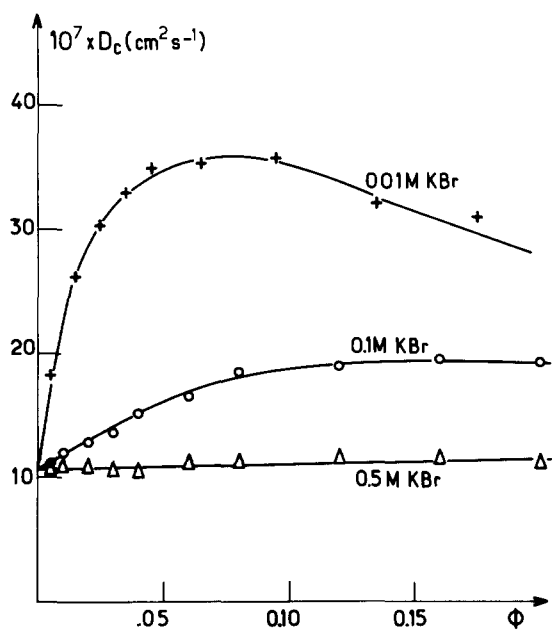

FIG. 2. QELS data: collective diffusion coefficients (D_c) vs volume fraction Φ. Symbols are defined in Fig. 1.

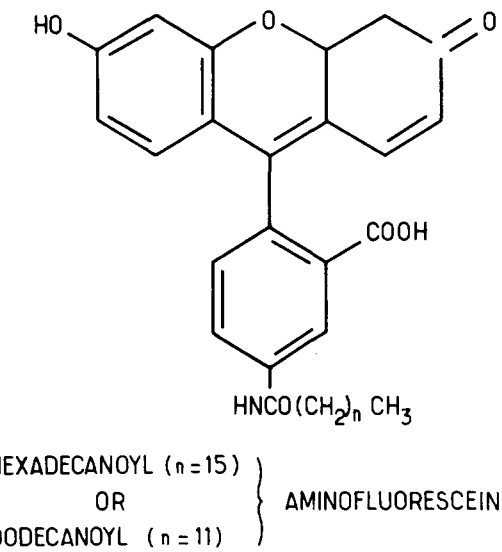

FIG. 3. Structure of the fluorescent dye used for self-diffusion experiments. Here we have chosen $n = 11$, i.e., the dodecanyl aminofluorescein.

C. Self-diffusion experiments

Since, in the case of micellar systems, optical experiments cannot probe the high-q regime in which self-diffusion coefficients can be obtained from quasielastic light scattering experiments, we have chosen to measure the long time self-diffusion coefficients by tracer diffusion. A very low amount (10^{-5} M/ℓ) of fluorescent dyes (Fig. 3) was added to the solutions. The dye has the same structure as a surfactant molecule: an aliphatic tail and a polar head (here the

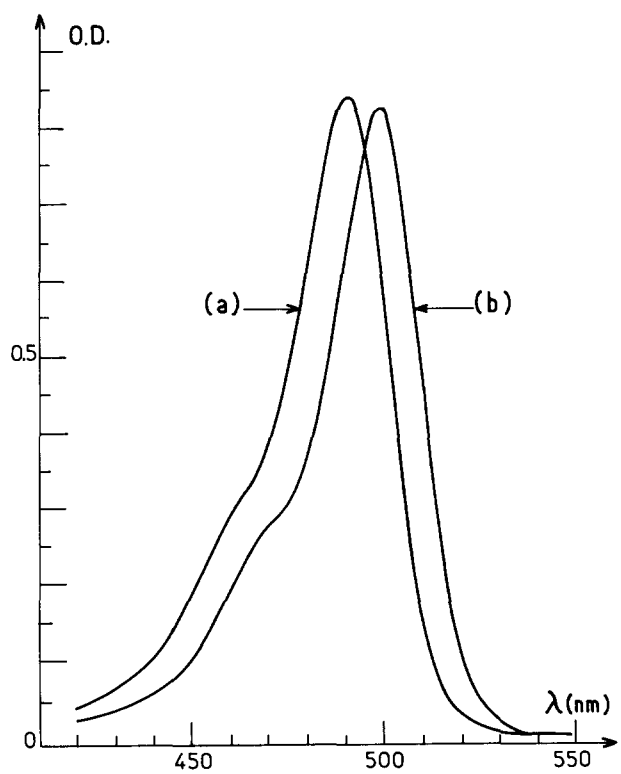

FIG. 4. Absorption spectra of the dye shown in Fig. 3. Curve (a) free dyes solubilized in water. Curve (b) dyes solubilized in micellar solution.

fluorescein group). Thus the dye molecule will be linked to micelles; this may be shown by fluorescence measurements. In Fig. 4 we give absorption spectra in two different situations; curve (a) is obtained in the case of free dyes in water, whereas curve (b) is obtained in presence of micelles. Though the shift of the absorption maximum is difficult to interpret, this clearly shows that, in micellar solutions, the dye is not solubilized as a free monomer but more probably linked to the micelles. This can be further proved by the measurement of the fluorescence steady state anisotropy, P; in the case of free dyes in water, one gets $P = 0.022$ whereas in the case of micellar solutions we obtain $P = 0.134$. This indicates that the dye is strongly immobilized within the micelles. Other evidence will be obtained from self-diffusion experimental results.

The fluorescence of the dye molecules can be destroyed by intense laser illumination. The principle of the experiment is then as follows. In a first step, we illuminate the sample with a high intensity fringe pattern produced by two crossed laser beams: this creates a nonuniform dye concentration distribution, since some of the dye molecules located in the bright fringes are irreversibly destroyed. Then the relaxation of this concentration profile is monitored with the same fringe pattern but of much weaker intensity in order not to keep on bleaching dyes. This monitoring is obtained by simply measuring the fluorescence intensity as a function of time. The long time self-diffusion coefficient is then obtained from the characteristic time τ of the fluorescence recovery curve:

$$D_S = \frac{i^2}{4\pi^2\tau},$$

where i is the fringe spacing. In order to increase the signal to noise ratio, we have used a phase modulated interferometer, which produces a modulated fluorescence signal detected by a lock-in amplifier.[35,36] The experimental setup we used is shown in Fig. 5. Diffusion coefficients easily measurable by this method are in the range 10^{-10}–10^{-5} cm^2 s^{-1}. For each

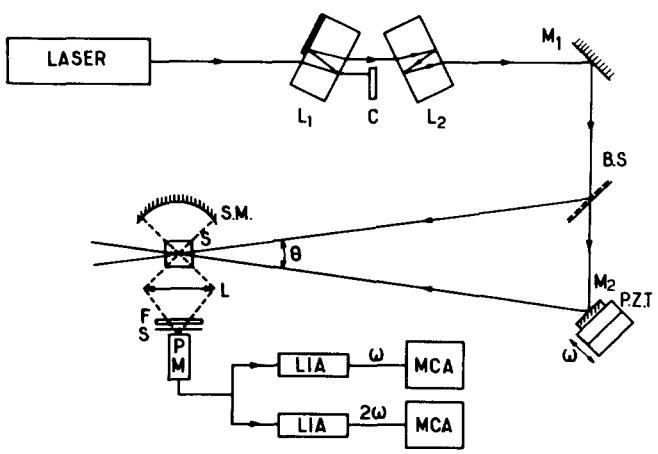

FIG. 5. Experimental setup used for self-diffusion experiments. The laser is an argon ion laser. L_1 and L_2: glass plates producing the two beams of unequal intensities. C: chopper. M_1 and M_2: mirrors. P.Z.T.: piezoelectric stack. S.M.: spherical mirror. L: high aperture lens. S: sample. F: filter centered at the fluorescence wavelength. S: shutter. L.I.A.: lock-in amplifier. M.C.A.: multichannel analyzer.

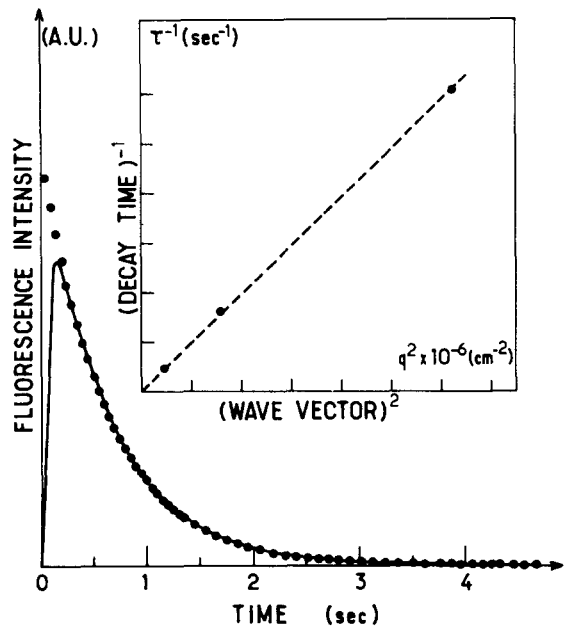

FIG. 6. Typical self-diffusion experimental results. The continuous line is the experimental curve obtained after averaging. The rise time is due to the lock-in amplifier time constant. Dots are obtained from fit of the experimental to a single exponential. In insert, we show the reciprocal recovery time τ^{-1} vs $q^2 = (2\pi/i)^2$.

sample, we performed three experiments at different values of the interfringe spacing (in the range 10–100 μm) in order to check the i^2 dependence of the fluorescence recovery characteristic time. Typical experimental results are given in Fig. 6. Each recovery curve was then fitted with a single exponential. This indicates that polydispersity effects are small as stated above. Before we give the results of these experiments, it is worthwhile to discuss in details the effects of dye exchanges between micelles on self-diffusion measurements. First of all a dye molecule can be exchanged between two colliding micelles; obviously this cannot affect self-diffusion measurements. A second process, which may affect the measured values of self-diffusion coefficients, is the dye transfer between two micelles through the solvent. Let T_R be the residence time of a dye in a micelle and T_D the time needed in order that the dye diffuses from one micelle to another. Typical value of T_R for 12 carbon atoms surfactant molecules[41] is 5 μs. Assuming micelles are immobile during T_D (which is justified in view of the respective diffusion coefficient of a monomer, $D_1 \sim 10^{-5}$ cm^2 s^{-1}, and a micelle, $D_m \sim 10^{-6}$ cm^2 s^{-1}), one gets

$$T_D = \frac{d^2}{6D_1},$$

where d is the average distance between micelles (see Sec. II A); for $\Phi \sim 1\%$, one has $d \sim 180$ Å and $T_D \sim 0.05$ μs. Since T_R and T_D are much smaller than the characteristic time τ of fluorescence recovery, one thus measures an average diffusion coefficient $\bar{D}$ given by

$$\bar{D} = \frac{T_R}{T_R + T_D} D_m + \frac{T_D}{T_R + T_D} D_1.$$

With the orders of magnitude given above for T_R and T_D the

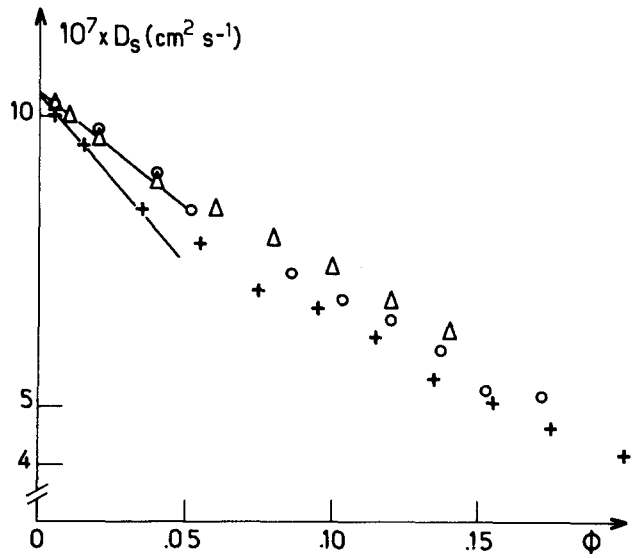

FIG. 7. Self-diffusion data: long time self-diffusion coefficients (D_S) vs volume fraction Φ. Symbols are defined in Fig. 1.

relative error on the measured value of the self-diffusion coefficient is about 10%. It should be noted that this effect decreases with concentration and will rapidly be of the order of experimental uncertainties (one obtains an error of about 5% for $\Phi = 3\%$). Furthermore the choosen value of T_R is probably underestimated; indeed the dye is certainly more hydrophobic than the surfactant used here (its solubility in water at 25 °C is less than 5.10^{-4} M/ℓ) and it has been shown that this may increase T_R by several orders of magnitude.[42] The results of self-diffusion experiments strongly support that the error on the measured value of the self-diffusion coefficients is indeed negligible (see Fig. 7 and Table I). We give in Table I the infinite dilution values of D_S (D_S^0), the hydrodynamic radii (R_H^{self}), and the first virial coefficients of D_S (α_S) for the three studied KBr concentrations. We observe that the agreement between the infinite dilution values of self and collective (D_c^0) diffusion coefficients is quite satisfactory; the above model suggests that the effect of dye exchanges should lead to an overestimation of D_S of about 20% for the lowest concentration studied here ($\Phi \sim 0.5\%$). Thus one may conclude that for these experiments, micelles behave like permanent spheres. Incidentally this agreement confirms two other points:

(1) The dye is effectively linked to the micelles.

(2) As QELS and FRAPP provide two different averages of diffusion coefficients (a number average for D_S and a z average for D_c), the polydispersity is really small.

In order to conclude, let us note that for systems very close to the c^* ($\Phi \sim 10^{-4}$), the fluorescence recovery curves exhibit two relaxation times: A short one which can be attributed to the dye free diffusion (from which we have evaluated D_1) and a long one from which one may extract a diffusion coefficient slightly larger than D_S^0 (by about 20%); for such a volume fraction, the above model suggests that one should measure an average diffusion coefficient three times greater than D_S^0. Again this clearly shows that we have underestimated T_R and that the finite residence time of the dye in the micelle has no effect on our results in the volume fraction range studied ($\Phi \geqslant 0.5\%$).

IV. DISCUSSION

Most of the results presented above are quite general in micellar systems.[12] For instance, we observe an increase in micellar aggregation number with salt concentration. This is fully understood in terms of geometrical models for surfactant aggregation and is accounted for by the decrease of polar heads areas due to the shielding of Coulombic repulsions between these polar heads.[37] It should be noted that for none of the studied salt concentrations we found evidence for structural changes in the explored surfactant concentration range. Since usually the addition of salt promotes micelle elongation, it is sufficient for our purpose to discuss only the case of 0.5 M KBr systems. As announced above (see Sec. II B 2), the polydispersity index stays low ($\sim 5\%$) in the whole studied concentration range; previous studies on the same type of cationic surfactants[38] have shown that micelle elongation is accompanied by a steep increase of the polydispersity index as measured by QELS. Furthermore, static light scattering data are interpreted exactly with a model of monodisperse hard spheres in the whole studied concentration range. This leads to the conclusion that at 0.5 M KBr micelles stay spherical up to 20% volume fraction and that it is also the case at 0.01 M and 0.5 M KBr as stated above about salt effect.

The low Φ behavior of both the collective diffusion coefficients and the scattered intensity are also in agreement with previous studies either on DTAB[38] or other surfactants.[12] Nevertheless, previous static light scattering studies were limited to low Φ. We have shown here that standard perturbation treatments may be used in order to account for the behavior of more concentrated solutions. This treatment allowed us to confirm low Φ data and to show that 0.5 M KBr solutions behave exactly like hard spheres. At this salinity, van der Waals attraction and Coulombic repulsions cancel each other.

In order to discuss the problem of collective and self-diffusion coefficients first virial, it may be remarked that we found a systematic discrepancy between the values of the mass and hydrodynamic radii (R and R_H in Table I). Since all theoretical calculations are done with $R = R_H$, it is not obvious to take into account these discrepancies. Nevertheless, one may introduce an "hydrodynamic volume fraction" Φ_H related to Φ by

$$\Phi_H = \Phi \left[\frac{R_H}{R} \right]^3. \tag{14}$$

Since the first virial coefficient (α_c) of D_c contains two contributions, direct interactions (B) and hydrodynamic ones (α_c'), one is thus led to correct only the contribution of hydrodynamic interactions in order to take into account the discrepancy between R and R_H

Expression (11) of the first virial coefficient of D_c, α_c becomes

$$\alpha_c = B - \left[\frac{\Phi_H}{\Phi} \right] \alpha_c'. \tag{15}$$

Using the values of Batchelor and Felderhof and the experimental results given in Table I for R and R_H, one would obtain $\alpha_c = -0.7$ for hard sphere-like systems, which has to be compared to the value obtained for the 0.5 M KBr systems given in Table I: $\alpha_c = 0 \pm 0.5$. Obviously this treatment is very crude and we will not try to extend this to the other salinities investigated here; nevertheless, such considerations may explain discrepancies between experiments and theoretical predictions. In the case of self-diffusion data, the same considerations lead this time to divide the α_S given in Table I by (Φ_H/Φ) in order to compare to theoretical results: This leads to $\alpha_S = -2.5 \pm 0.5$ for 0.5 M KBr, $\alpha_S = -2.4 \pm 0.5$ for 0.1 M KBr, and $\alpha_S = -2 \pm 0.5$ for 0.01 M KBr. At this point, experimental data do not allow to decide clearly between all predicted values of α_S but seem to favor those which assume that changes in D_S are due to increased friction coefficient,[39] predicting $\alpha_S = -2.5$ for hard spheres. The examination of Fig. 7 clearly shows that, as expected (see Sec. II B 2), D_S does not strongly depend upon direct interactions.

At this point, it is worthwhile to discuss a problem linked to the two friction coefficients f_c and f_S, which appear in the definitions (7) and (8) of, respectively, the collective and self-diffusion coefficients. It has often been believed that these two friction coefficients were equal.[18,40] Indeed the author of Ref. 18 suggests that the bulk of available experimental data are in favor of this equality.

If this were true, among the three quantities I, D_c and D_S, only two would be independent. From Eqs. (1), (7), and (8), one may calculate the ratio

$$\frac{f_c}{f_S} \propto \frac{D_S}{D_c} \cdot \frac{\Phi}{I}. \tag{16}$$

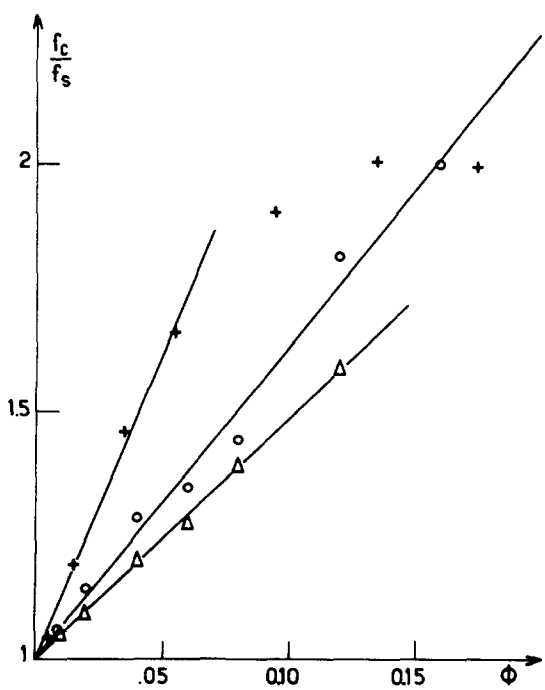

FIG. 8. Comparison between collective (f_c) and self- (f_s) friction coefficients. Plot of the ratio f_c/f_s [cf. Eq. (16)] vs volume fraction (Φ). Symbols are defined in Fig. 1.

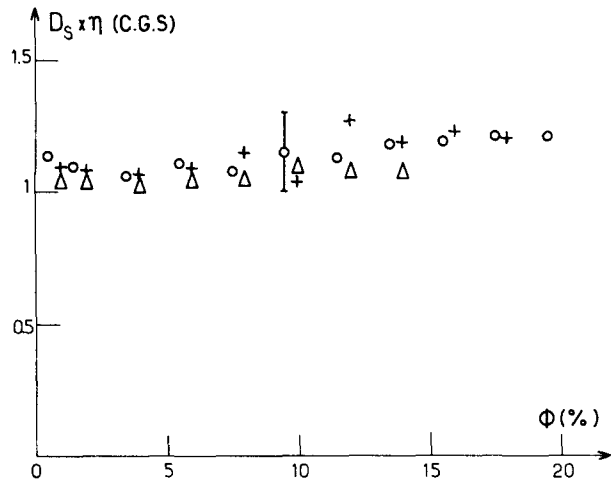

FIG. 9. Comparison of viscosity and self-diffusion data. Plot of the product ηD_S vs volume fraction. Symbols are defined in Fig. 1.

If f_c and f_S were equal, this ratio should be independent of Φ. Since we have measured, for three distinct systems, the three quantities, it is easy to test this hypothesis. This is done in Fig. 8, where we have plotted f_c/f_S against Φ. Clearly, we definitely do not have $f_c = f_S$ even for moderately concentrated systems which is in agreement with theoretical predictions.[6,19]

Finally, one may also compare the micelles self-diffusion coefficient to the viscosity of the micellar solutions. Indeed it is well known that for simple liquids one has ηD_S constant[43] with η, the liquid viscosity, and D_S, the molecular self-diffusion coefficient. This fact seems to have firm theoretical basis in that case.[44] In Fig. 9, we show the product ηD_S for the micellar systems we have studied (η was measured with a capillary viscosimeter). Obviously, one has the same type of properties in that case too, namely ηD_S is constant. This has already been observed in the case of monodisperse latex spheres in water[45] and in some microemulsion systems.[47] It seems that this relation between viscosity and self-diffusion coefficients has received little attention in the case of colloidal suspensions and lacks firm theoretical basis. Nevertheless, this result confirms that colloidal suspensions are really "colloidal liquids" as suggested by their previously studied static and dynamic properties.

V. CONCLUSION

We have presented very complete data on DTAB micellar systems at three different salinities: osmotic compressibility, mutual, and self-diffusion coefficients, as measured with light scattering and fluorescence photobleaching experiments. The data have been fitted with existing theories. Extrapolations to zero droplet volume fraction give masses and hydrodynamic radii. Sizes increase with water salinity as usual. When the water salinity is large enough, scattered light intensity exhibits a peak around droplet volume fractions at 10%. A classical treatment adding small perturbations to a hard sphere potential, proposed by Vrij in the case of microemulsions, has been applied to a micellar system. It gave us the hard sphere radii of the micelles. Hard sphere

and mass radii are very close. The difference between hard sphere and hydrodynamic radius is about 2 Å. It corresponds to the thickness of water hydration layer. Let us point out that the only other way to directly measure this thickness is neutron (or x ray) scattering experiments. Light scattering experiments are of course easier to perform.

Virial coefficients have also been measured. They correspond to strongly repulsive interactions at low salinity, and hard sphere + moderately repulsive interactions at higher salinities. For 0.5 M salt, the electrostatic repulsion is balanced by van der Waals attraction and the system is hard sphere-like. Such evolution strongly affects the light scattering features as already reported by former authors on similar systems. We show here that self-diffusion is almost insensitive to interactions between micelles as predicted theoretically.

Finally, we clearly show that the friction coefficients involved in mutual and self-diffusion have different variations with droplet volume fraction.

ACKNOWLEDGMENTS

It is a pleasure to thank R. Klein, J. Lang, J. Meunier, and R. Zana for fruitful discussions. This work received financial support from PIRSEM (GRECO "Microemulsions").

[1]G. K. Batchelor, J. Fluid. Mech. **74**, 1 (1976).
[2]B. J. Ackerson, J. Chem. Phys. **69**, 684 (1978).
[3]B. U. Felderhof, J. Phys. A **11**, 929 (1978).
[4]C. W. J. Beenakker and P. Mazur, Phys. Lett. A **91**, 290 (1982).
[5]S. Walrand, L. Belloni, and M. Drifford, J. Phys. (Paris) **47**, 1565 (1986).
[6]W. Dietrich and J. Peschel, Physica A **94**, 208 (1975).
[7]F. Grüner and W. Lehmann, in *Light Scattering in Liquids and Macromolecular Solutions*, edited by V. Degiorgio, M. Corti, and M. Giglio (Plenum, New York, 1980), p. 51.
[8]P. N. Pusey, J. Phys. A **11**, 119 (1978).
[9]P. Doherty and G. B. Benedek, J. Chem. Phys. **61**, 5426 (1975).
[10]A. M. Cazabat and D. Langevin, J. Chem. Phys. **74**, 3148 (1981).
[11]N. A. Mazer, G. B. Benedek, and M. C. Carey, J. Phys. Chem. **80**, 1075 (1976).
[12]M. Corti and V. Degiorgio, J. Phys. Chem. **85**, 711 (1981).
[13]E. A. G. Anianson, Progr. Colloid Polymer Sci. **70**, 2 (1985).
[14]G. T. Evans and C. P. James, J. Chem. Phys. **79**, 5553 (1983).
[15]M. Venkatesan, C. S. Hirtzel, and R. Rajagopalan, J. Chem. Phys. **82**, 5685 (1985).
[16]N. Yoshida, J. Chem. Phys. **83**, 4786 (1985).
[17]P. N. Pusey and W. van Megen, J. Phys. (Paris) **44**, 285 (1983).
[18]G. D. J. Phillies, Macromolecules **17**, 2050 (1984).
[19]A. R. Altenberger and M. Tirrell, J. Polym. Sci. **22**, 909 (1984).
[20]P. N. Pusey, J. Phys. A **8**, 1433 (1975).
[21]L. I. Komarov and J. Z. Fisher, Sov. Phys. JETP **16**, 1358 (1963).
[22]C. Tanford, *Physical Chemistry of Macromolecules* (Wiley, New York, 1961), p. 275.
[23]A. A. Calje, W. G. M. Agterof, and A. Vrij, in *Micellization, Solubilization and Microemulsions* (Plenum, New York, 1977), Vol. 2, p. 779.
[24]N. F. Carnahan and K. E. Sterling, J. Chem. Phys. **51**, 635 (1969).
[25]E. J. W. Verwey and J. T. G. Overbeck, *Theory of the Stability of Iyophobic Colloids* (Elsevier, New York, 1948).
[26]J. M. Carter and G. D. J. Phillies, J. Phys. Chem. **89**, 5118 (1985).
[27]W. van Megen, I. Snook, and P. N. Pusey, J. Chem. Phys. **78**, 931 (1983).
[28]C. W. Beenakker and P. Mazur, Physica A (Amsterdam) **120**, 388 (1983).
[29]P. Mazur and W. van Saarloos, Physica A (Amsterdam) **115**, 21 (1982).
[30]J. M. Corkill, J. F. Goodman, and T. Walker, Trans. Faraday Soc. **63**, 768 (1967).
[31]J. Lang and R. Zana (to be published).
[32]M. Kerker, *The Scattering of Light and Other Electromagnetic Radiation* (Academic, New York, 1969), p. 543.
[33]P. N. Pusey, in *Photon Correlation and Light Beating Spectroscopy*, edited by H. Z. Cummins and E. R. Pike (Plenum, New York, 1974), p. 387.
[34]Although, in our case, the characteristic decay times of the correlation functions are comparable to the "local structure renewal time" τ_I, because of the q^{-2} dependence of these decay times and the agreement between hydrodynamic radii determined by QELS and FRAPP, we believe that D_c is actually measured. Furthermore, in case of 0.5 and 0.1 M KBr systems, repulsive interactions are weak so that memory effects should be weak too.
[35]J. Davoust, P. F. Devaux, and L. Leger, EMBO J. **1**, 1233 (1982).
[36]D. Chatenay, W. Urbach, A. M. Cazabat, and D. Langevin, Phys. Rev. Lett. **54**, 2253 (1985).
[37]J. N. Israelachvili, D. J. Mitchell, and B. W. Ninham, J. Chem. Soc. Faraday Trans. 2 **72**, 1525 (1976).
[38]S. J. Candau, E. Hirsch, and R. Zana, J. Phys. (Paris) **45**, 1263 (1984).
[39]A. Einstein, *Investigations on the Theory of Brownian Motion* (Dover, New York, 1956).
[40]G. M. Trotter and D. N. Pinder, J. Chem. Phys. **75**, 118 (1981).
[41]E. A. G. Aniansson, S. N. Wall, M. Almgren, H. Hoffmann, I. Kielman, W. Ulbricht, R. Zana, J. Lang, and C. Tondre, J. Phys. Chem. **80**, 905 (1976).
[42]J. D. Bolt and N. J. Turro, J. Phys. Chem. **85**, 4029 (1981).
[43]H. J. Parkhurst, Jr. and J. Jonas, J. Chem. Phys. **63**, 2698 (1975).
[44]R. Zwanzig, J. Chem. Phys. **79**, 4507 (1983).
[45]W. D. Dozier, H. M. Lindsay, and P. M. Chaikin, J. Phys. (Paris) C3 **46**, 165 (1985).
[46]A. M. Cazabat, D. Chatenay, D. Langevin, J. Meunier, and L. Léger, in *Surfactant in Solutions*, edited by K. L. Mittal and B. Lindman (Plenum, New York, 1984).
[47]L. B. Bangs, in Technical Notice, Seragen Diagnostics Inc., 1984.